e-J. Surf. Sci. Nanotech. Vol. 13 (2015) 27-30 Conference - CIF'15 -

Synthesis and Photoluminescence Properties of Nonanuclear Tb(III) Clusters with Long Alkyl Chain Group*

Shun Omagari, Takayuki Nakanishi,† Yuichi Kitagawa, Koji Fushimi, and Yasuchika Hasegawa‡
Faculty of Engineering, Hokkaido University, N13 W8, Kita-ku, Sapporo, Hokkaido 060-8628, Japan.
(Received 25 December 2014; Accepted 24 January 2015; Published 14 February 2015)

Series of nonanuclear Tb(III) clusters with ligands of different length of alkyl chain groups and their photophysical properties are demonstrated. The nonanuclear Tb(III) clusters (Tb_9 clusters) are composed of nine oxygen-bridged Tb(III) ions and sixteen alkyl salicylate ligands, where alkyl chain are ethyl (Tb_9-Et), propyl (Tb_9-Pr), butyl (Tb_9-Bu), and hexyl (Tb_9-Hex) groups. The luminescence properties of the Tb_9 clusters are characterized by absorption spectra, emission quantum yields, and emission lifetimes. The radiative (k_r) and nonradiative (k_{nr}) rate constants were calculated from their photophysical properties. Tb_9-Hex have shown the highest k_r (859 s^{-1}) and lowest k_{nr} (137 s^{-1}), owing to the tight packing due to CH-π interaction by long alkyl chains.
[DOI: 10.1380/ejssnt.2015.27]

Keywords: Photoluminescence; Lanthanides; Clusters

I. INTRODUCTION

Lanthanide complexes have attracted much attention during the past two decades for their brilliant luminescence of trivalent lanthanide ions that possess many intrinsic properties such as narrow emission band and long emission lifetimes of millisecond order. As commonly known, lanthanide complexes are composed of lanthanide ion and organic ligands. The electronic transitions between the 4f orbitals are forbidden, leading to small absorption coefficient [1]. The use of organic ligand with high absorption coefficient as light-harvesting "antenna" [2,3] is an effective method for achieving intense luminescence of lanthanide ions. Such intense luminescence makes them one of the possible candidates for practical application to e.g. light-emitting diodes [4], light-converters [5], and bioassays [6].

In order to maximize the luminescence efficiency of lanthanide complexes, two considerable approaches are commonly accepted [7,8]. The one is suppressing nonradiative rate constant k_{nr} and the other is enhancing radiative rate constant k_r. The radiative rate constants k_r observed for lanthanide complexes greatly depend on the geometrical symmetry of the coordination structure. Lima *et al.* has demonstrated that the distortion of coordination geometry of lanthanide ion leads to high emission quantum yields [7]. We have also reported that the asymmetric dodecahedron structure give rise to high k_r [9]. These results indicate that the radiative transition probability between the $4f$ orbitals is enhanced by reducing the geometrical symmetry of the coordination structures. On the other hand, the emission properties of lanthanide complexes also depend on their vibrational structures, which dominate the kinetics of nonradiative transitions. According to the energy-gap law, nonradiative transitions are promoted by ligands and solvents with high-frequency vibrational structures. For these reasons, lanthanide complexes with large k_r and small k_{nr} constants are the most favorable for strongly luminescent material.

We have reported nonanuclear Tb(III) clusters with two characteristic asymmetric coordination geometry. The Tb(III) clusters possess one 8-coordinate square-antiprism (8-SAP) and eight 8-coordinate trigonal-dodecahedron (8-TDH) structures [10]. The nonanuclear Tb(III) clusters contain a Tb(III) ion-rich core bridged by oxygen atoms, with sixteen alkyl salicylate ligands coordinating around that core. The Tb(III) cluster also contain systematic intramolecular CH-π and π-π interactions. The intramolecular interactions can be changed using alkyl salicylate derivatives that affects coordination geometry of Tb(III) ions [7,9,11]. In terms of the photophysical properties coordination geometry has strong relationship with photophysical properties.

In this study, we synthesized a series of nonanuclear Tb(III) clusters, $[Tb_9(\text{alkyl-salicylate})_{16}(\mu\text{-OH})_{10}]^+NO_3^-$, where linear alkyl chain groups ($-C_nH_{2n+1}, n = 2, 3, 4, 6$) are introduced to the alkyl part of the salicylate derivatives. The photophysical properties were investigated by emission and absorption spectroscopy, absolute quantum yield measurements, and emission lifetime. This paper discusses the relationship between the difference in coordination geometry and photophysical properties in Tb(III) clusters for the first time.

II. EXPERIMENTAL

A. Synthesis of Tb_9 clusters ($[Tb_9(\text{alkyl salicylate})_{16}(\mu\text{-OH})_{10}]^+NO_3^-$)

General synthesis procedures are shown in Scheme 1. Appropriate alkyl salicylate (2.7 mmol) was dissolved in methanol and triethylamine (0.44 ml, 4.40 mmol) was added to this solution with stirring at 40°C. Then, $Tb(NO_3)_3{\cdot}6H_2O$ (0.686 g, 1.52 mmol) in methanol was added dropwise to this solution with further stirring for 20 min. White powder, $[Tb_9(\text{alkyl salicylate})_{16}(\mu\text{-OH})_{10}]^+NO_3^-$, was obtained.

* This paper was presented at the 15th Chitose International Forum "Nanotechnology - From Synthesis to Devices," Chitose Institute of Science and Technology, Chitose, Japan, October 2-3, 2014.
† Corresponding author: nakanishi@eng.hokudai.ac.jp
‡ Corresponding author: hasegaway@eng.hokudai.ac.jp

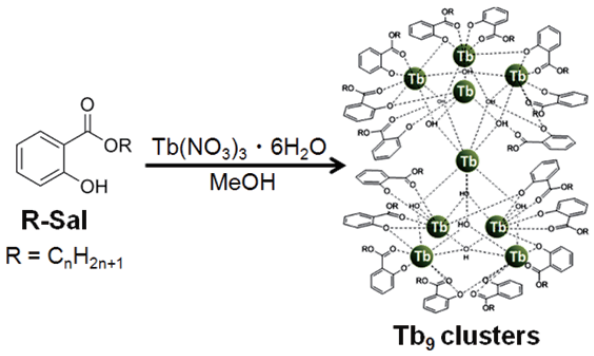

SCHEME 1. General procedures for synthesis of Tb_9 clusters.

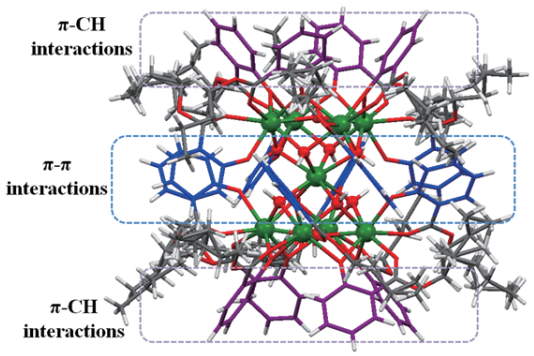

FIG. 1. Molecular structure of Tb_9–Bu [10]. The intramolecular π-π and CH-π interactions are emphasized in blue and violet dotted lines.

B. Synthesis of Tb_9–Et ($[Tb_9(Et–Sal)_{16}(\mu\text{-}OH)_{10}]^+NO_3^-$)

Elemental analysis calculated for $C_{144}H_{154}NO_{61}Tb_9$: C, 40.17%, H, 3.61%, N, 0.33%. Found: C, 39.91%, H, 3.59%, N , 0.34%. FAB-MS: m/z 4242.2 $[Tb_9(Et–Sal)_{16}(\mu\text{-}OH)_{10}]^+$.

C. Synthesis of Tb_9–Pr ($[Tb_9(Pr–Sal)_{16}(\mu\text{-}OH)_{10}]^+NO_3^-$)

Elemental analysis calculated for $C_{160}H_{186}NO_{61}Tb_9$: C, 42.43%, H, 4.14%, N, 0.31%. Found: C, 42.12%, H, 4.10%, N , 0.34%. FAB-MS: m/z 4466.6 $[Tb_9(Pr–Sal)_{16}(\mu\text{-}OH)_{10}]^+$.

D. Synthesis of Tb_9–Bu ($[Tb_9(Bu–Sal)_{16}(\mu\text{-}OH)_{10}]^+NO_3^-$)

Elemental analysis calculated for $C_{176}H_{218}NO_{61}Tb_9$: C, 44.47%, H, 4.62%, N, 0.29%. Found: C, 44.16%, H, 4.57%, N, 0.51%. FAB-MS: m/z 4691.3 $[Tb_9(Bu–Sal)_{16}(\mu\text{-}OH)_{10}]^+$.

E. Synthesis of Tb_9–Hex ($[Tb_9(He–Sal)_{16}(\mu\text{-}OH)_{10}]^+NO_3^-$)

Elemental analysis calculated for $C_{208}H_{282}NO_{61}Tb_9$: C, 48.02%, H, 5.46%, N, 0.27%. Found: C, 47.8%, H, 5.28%, N, 0.31%. FAB-MS: m/z 5140.0 $[Tb_9(He–Sal)_{16}(\mu\text{-}OH)_{10}]^+$.

F. Optical Measurements

All measurements for the Tb(III) clusters were done in chloroform solution. UV/Vis absorption spectra (1.0×10^{-4} M) were recorded using JASCO V-660 spectrometer. Emission spectra was recorded using Horiba FluoroLog3. Emission lifetimes (τ_{obs}, 1.0×10^{-4} M) were measured using the third harmonics (355 nm) of a Q-switched Nd:YAG laser (Spectra Physics, INDI-50, fwhm = 5 ns, $\lambda = 1064$ nm) and a photomultiplier (Hamamatsu photonics, R5108, response time $\leq$ 1.1 ns). The Nd:YAG laser response was monitored with a digital oscilloscope (Sony Tektronix, TDS3052, 500 MHz) synchronized to the single-pulse excitation. Emission lifetimes were determined from the slope of logarithmic plots of the decay profiles.

The absolute emission quantum yields excited at 380 nm ($\Phi_{\pi\pi^*}$, 1.0×10^{-4} M) and 488 nm (Φ_{ff}, 1.0×10^{-2} M) were estimated using JASCO F-6300-H spectrometer attached with JASCO ILF-533 integrating sphere unit ($\phi = 100$ mm). The wavelength dependences of the detector response and the beam intensity of Xe light source for each spectrum were calibrated using a standard light source. Quantum yield can be calculated by $[\Phi = (E_c - E_a)/(L_a - L_c)]$ with E_c being the integrated emission spectrum of the sample, E_a the integrated "blank" emission spectrum, L_a the "blank" absorption, and L_c the sample absorption at the excitation wavelength.

III. RESULTS AND DISCUSSION

Identification of the Tb_9 clusters was performed by fast-atomic bombardment mass spectroscopy (FAB-MS). The m/z for Tb_9–Et, Tb_9–Pr, Tb_9–Bu, Tb_9–Hex were determined to be 4242.2, 4466.6, 4691.3, and 5140.0, respectively. The obtained m/z can be attributed to Tb_9 clusters without the NO_3^- counter-anion. The molecular structures of the Tb_9 clusters are given in our previous report by single-crystal X-ray measurements [10]. The Tb_9 clusters possess nine oxygen-bridged Tb(III) ions with a "sand-glass" structure surrounded by sixteen alkyl salicylate ligands as shown in Fig. 1. The packing structure of the Tb_9 clusters can be explained by systematic intramolecular CH-π and π-π interactions between ligands. The π-π interactions are observed between two aromatic rings ($\sim$ 4.25 Å) near the center of the cluster. The CH-π interactions are also found between alkyl chain and aromatic ring ($>$ 2.75 Å) near the top and bottom of the cluster [10]. We successfully obtained four nonanuclear Tb(III) clusters, Tb_9-Et, Tb_9-Pr, Tb_9-Bu, and Tb_9-Hex.

Absorption spectra of ligands and Tb_9 clusters in 1.0×10^{-5} M chloroform are shown in Fig. 2a and 2b, respectively. Tb_9-Bu showed the largest absorption coefficient

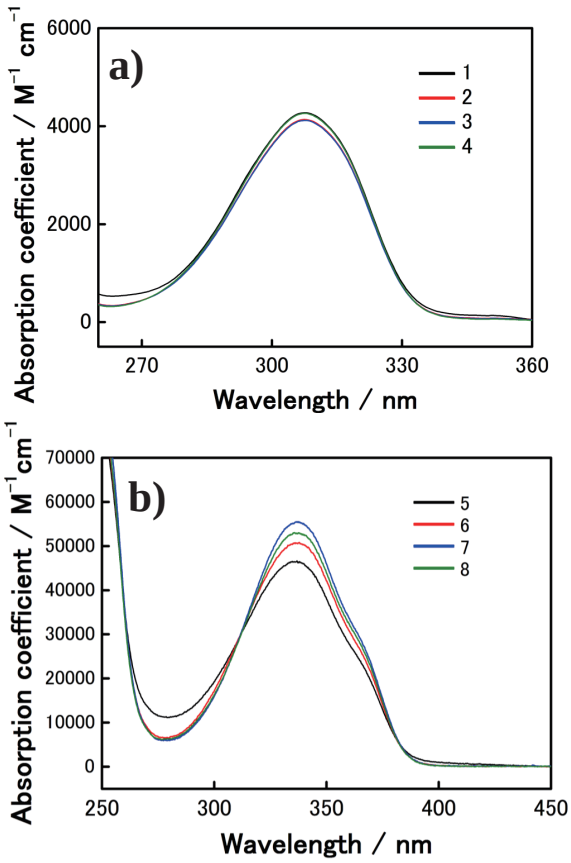

FIG. 2. Absorption spectra of (a) alkyl salicylate ligands and (b) Tb_9 clusters. 1) Tb_9-Et, 2) Tb_9-Pr, 3) Tb_9-Bu, and 4) Tb_9-Hex.

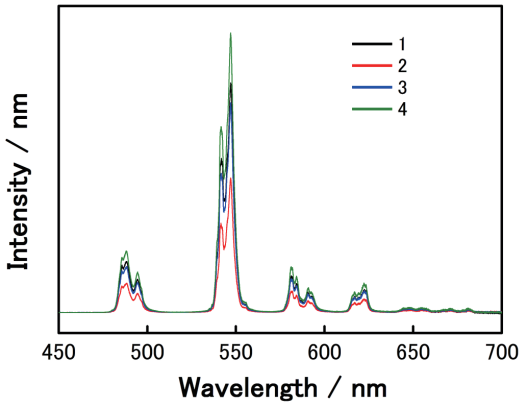

FIG. 3. Emission spectra of Tb_9 clusters. 1) Tb_9–Et, 2) Tb_9–Pr, 3) Tb_9–Bu, and 4) Tb_9–Hex.

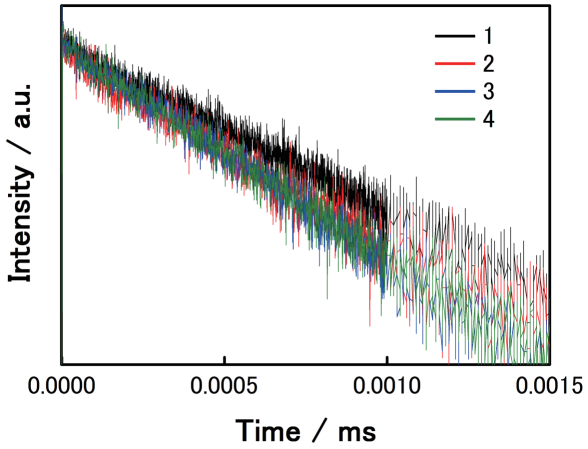

FIG. 4. Emission lifetimes of Tb_9 clusters. 1) Tb_9-Et, 2) Tb_9-Pr, 3) Tb_9-Bu, and 4) Tb_9-Hex.

of 55508 M^{-1} cm^{-1} while Tb_9-Et showed the smallest absorption coefficient of 46432 M^{-1} cm^{-1}. Difference in absorption coefficient is observed for the Tb_9 clusters with different alkyl chain, but there is no proportional relationship between the length of alkyl chain and the absorption coefficient. We suggest that the oscillator strength can be modified using intramolecular interactions. Emission spectra of the Tb_9 clusters in 1.0×10^{-4} M chloroform are shown in Fig. 3. Emission bands of the Tb_9 clusters are observed at approximately 487, 548, 582, 623, 651, and 681 nm, which are attributed to the $4f$–$4f$ transition of Tb(III) ions ($^5D_4$–^7F_J ($J = 6 - 1$)). The difference in peaks is derived from the different absorbance excited at 480 nm ex.

The emission decay profiles and their specific values τ_{obs} of Tb_9 clusters are shown Fig. 4 and Table I, respectively. The emission lifetimes were determined from the slopes of the logarithmic plots of the decay profiles. The longest τ_{obs} was obtained for Tb_9-Et (1.26 ms) while the shortest was Tb_9-Hex (1.00 ms). Table I shows that the quantum yields by ligand excitation at 380 nm ($\Phi_{\pi\pi^*}$) of the clusters are at around 40%. Quantum yields by Tb(III) ion excitation at 487 nm (Φ_{ff}) are quite different from 42% to 86%. Radiative (k_r) and nonradiative (k_{nr}) rate constant were calculated from quantum yield excited at 488 nm and emission lifetimes. As shown in Table I, steady decrease in k_r and increase in k_{nr} can be observed from Tb_9-Et (k_r = 548 s^{-1}, k_{nr} = 246 s^{-1}) to Tb_9-Bu (k_r = 358 s^{-1}, k_{nr} = 497 s^{-1}). However, Tb_9-Hex showed significantly large k_r (859 s^{-1}) and small k_{nr} (137 s^{-1}) compared to other clusters. This is likely due to the difference in the length of the alkyl chain that systematically affects the CH-π and π-π interactions which leads to difference in packing structure of the Tb_9 cluster. While increase in the length of alkyl chain increases quenching sites (C–H vibration), we suggest that when the length of alkyl chain is long enough, the packing structure may be optimized leading to large k_r and small k_{nr}.

IV. CONCLUSIONS

A series of nonanuclear Tb(III) clusters with different alkyl length on salicylate derivatives, Tb_9-Et, Tb_9-Pr, Tb_9-Bu, and Tb_9-Hex has been synthesized and characterized by their photophysical properties. The photophys-

TABLE I. Photophysical properties of Tb(III) complexes

Tb_9 cluster	$\epsilon_{\pi\pi^*}/M^{-1}\ cm^{-1}$	$\Phi_{\pi\pi^*}$	Φ_{ff}	η_{sens}	τ_{obs}/ms	τ_{rad}/ms	k_r/s^{-1}	k_{nr}/s^{-1}
Tb_9-Et	46432	42%	69%	61%	1.26	1.82	548	246
Tb_9-Pr	50665	40%	56%	72%	1.13	2.03	493	392
Tb_9-Bu	55508	39%	42%	93%	1.17	2.79	358	497
Tb_9-Hex	52897	42%	86%	49%	1	1.16	859	137

ical properties depend on the length of the alkyl chain of the ligands. While $\Phi_{\pi\pi^*}$ were around 40% for the Tb_9 clusters, Φ_{ff} were much different ranging from 42% of Tb_9-Bu to 87% of Tb_9-Hex. Tb_9-Hex has shown the largest k_r ($859\ s^{-1}$) and smallest k_{nr} ($137\ s^{-1}$). We consider that the length of the alkyl chain of the ligands will affect the CH-π and π-π interactions, which systematically changes the packing structure of the clusters. We conclude that the packing structure could lead to characteristic photophysical properties of the clusters.

ACKNOWLEDGMENTS

This work was supported by Frontier Chemistry Center Akira Suzuki "Laboratories for Future Creation" Project.

[1] L. Armelao, S. Quici, F. Barigelletti, G. Accorsi, G. Bottaro, M. Cavazzini, and E. Tondello, Coord. Chem. Rev. **254**, 487 (2010).
[2] L. Smentek and A. Kedziorski, J. Lumin. **130**, 1154 (2010).
[3] J.-C. G. Bünzli and C. Piguet, Chem. Soc. Rev. **34**, 1048 (2005).
[4] T. Oyamada, Y. Kawamura, T. Koyama, H. Sasabe, and C. Adachi, Adv. Mater. **16**, 1082 (2004).
[5] G. F. De Sá, O. L. Malta, C. de Mello Donegá, A. M. Simas, R. L. Longo, P. A. Santa-Cruz, and E. F. da Silva Jr., Coord. Chem. Rev. **196**, 165 (2000).
[6] R. A. Poole, F. Kielar, S. L. Richardson, P. A. Stenson, and D. Parker, Chem. Commun. **4084** (2006).
[7] N. B. D. Lima, S. M. C. Gonçalves, S. A. Júnior, and A. M. Simas, Sci. Rep. **3**, 2395 (2013).
[8] Y. Hasegawa, Y. Wada, and S. Yanagida, J. Photochem. Photobiol. C Photochem. Rev. **5**, 183 (2004).
[9] Y. Hasegawa, T. Ohkubo, T. Nakanishi, A. Kobayashi, M. Kato, T. Seki, H. Ito, and K. Fushimi, Eur. J. Inorg. Chem. **5911** (2013).
[10] T. Nakanishi *et al.*, Inorg. Chem. **53**, 7635 (2014).
[11] K. Miyata, T. Nakagawa, R. Kawakami, Y. Kita, K. Sugimoto, T. Nakashima, T. Harada, T. Kawai, and Y. Hasegawa, Chem. Eur. J. **17**, 521 (2011).